

Zirconium phosphate/phosphonate multilayered films based on push–pull stilbazolium salt: synthesis, characterization and second harmonic generation

Tamara Morotti,^a Valentina Calabrese,^a Marco Cavazzini,^a Danilo Pedron,^b Matteo Cozzuol,^b Antonino Licciardello,^c Nunzio Tuccitto^c and Silvio Quici^{*a}

Received 22nd January 2008, Accepted 25th March 2008

First published as an Advance Article on the web 24th April 2008

DOI: 10.1039/b801194j

The preparation of materials featuring enhanced second harmonic generation (SHG) values by self-assembly of molecules characterized by high second-order non-linear optic (NLO) activity is nowadays an important and challenging field of research. In order to show SHG the material must have an acentric structure with the dipoles of the molecular components oriented in the same direction and this is synthetically fairly difficult to achieve. This study describes the synthesis of the push–pull stilbazolium salt **1** and its assembly in multilayered acentric thin films, on quartz glass surface, by using the zirconium phosphate/phosphonate (Zr-PO_x) technique. A particular care has been paid to the optimization of the surface preparation and of the deposition conditions. This allows to obtain highly homogeneous lamellar inorganic–organic materials showing satisfactory second harmonic generation (SHG) values together with high chemical, thermal and mechanical stabilities which are necessary for their integration in optoelectronic devices.

Introduction

Nowadays the preparation of functional and multifunctional devices by nano-organization of single molecular components represents a demanding goal in the development of nanoscience and nanotechnology.^{1,2} In particular, in recent years increasing efforts have been focused on materials showing high second harmonic generation (SHG) values, which are prepared from second-order non-linear optical (NLO) organic molecules. These materials could find application in many fields such as telecommunications, data storage and processing and laser technologies and in perspective could efficiently replace usually exploited inorganic matrices.³ It is well known that high second-order NLO activity is observed in dipolar compounds characterized by the presence of an electron-donating and an electron-withdrawing group connected by π -conjugated linker “push–pull molecules”.⁴ For this reason materials showing high SHG values should feature an acentric structure which means that the dipole moment of molecular components should be oriented in the same direction.

To this end, several nano-organization techniques have been developed, for instance growing of non-centrosymmetric molecular crystals,⁵ inclusion of NLO compounds into organic or inorganic guest,^{6,7} electric field induced poling of polymer⁸ and hydrogen-bonding assisted physical vapour deposition (PVD).⁹ Moreover the “layer by layer” approaches towards the preparation of non-linear optic materials seem to be the most

promising, e.g.: Langmuir–Blodgett films,¹⁰ layered cationic–anionic polymer,¹¹ trifunctionalized siloxane¹² and zirconium phosphate/phosphonate (Zr-PO_x) technique.¹³ In these cases, an appropriate design of the molecular organic components ensures a rigid control over their alignment on the substrate surface. The Zr-PO_x technique is based on the consideration that organic phosphonic acids form highly insoluble, layered salts with Zr(IV) and other transition metals.¹⁴ By using this procedure Mallouk and co-workers showed that a series of different bis-phosphonic acids could be assembled as Zr(IV) salts on a substrate one layer at time and that this iterative method allowed to reproduce on the surface the lamellar structure of the Zr(IV) phosphate/phosphonate salt.^{15–17} A few years later Katz and co-workers, at the AT & T Bell Laboratories, by using a modification of Mallouk’s method assembled a family of push–pull azo-dyes into noncentrosymmetric multilayer films.¹³ The key of the sequential deposition technique used by Katz *et al.* has been to design a three-step adsorption sequence involving molecules with a phosphonate group in one end and a hydroxyl at the other. The three steps are: chemisorption of the phosphonate end of the molecule on the Zr⁴⁺ phosphate layer, phosphorylation of the exposed hydroxyl group with POCl₃ to afford phosphate and zirconation of the latter to regenerate the surface. The reiteration of this sequence led to multilayered hybrid organic/inorganic films that showed second-order non-linear optic coefficients of the same order of magnitude of LiNbO₃ together with very high chemical, mechanical and thermal stabilities, which are prerequisites for their integration in optoelectronic devices. In this paper, together with the synthesis of the stilbazolium salt **1** and the preparation of oriented multilayers by self-assembly with the Zr-PO_x technique, a particular attention has been paid to the improvement of deposition parameters that are essential for the reproducibility of the materials either from the structural or functional point of view.

^aCNR - Istituto di Scienze e Tecnologie Molecolari, Via C. Golgi 19, 20133, Milano, Italy. E-mail: silvio.quici@istm.cnr.it; Fax: +39-02-50314159; Tel: +39-02-50314164

^bDipartimento di Scienze Chimiche, Università di Padova, Via Marzolo 1, 35131, Padova. E-mail: danilo.pedron@unipd.it; Fax: +39-049-8275135; Tel: +39-049-8275121

^cDipartimento di Scienze Chimiche, Università di Catania, Viale A. Doria 6, 95125, Catania, Italy. E-mail: alicciardello@dipchi.unict.it; Fax: +39-095-580138; Tel: +39-095-7385086

Results and discussion

Synthesis of the chromophore 1

The stilbazolium salt **1** (Scheme 1) has been designed in order to allow the deposition of one Zr-PO_x monolayer at a time. Indeed it contains a phosphonic group, at one end of the molecule, which is ready for binding with the surface functionalized with zirconium phosphate, and a primary hydroxyl group on the other end that can be easily converted to a phosphate residue after phosphorylation with POCl₃. In comparison with the push-pull azo-dyes reported by Katz and co-workers¹³ the stilbazolium salt **1** should show an enhanced second-order NLO activity because of the presence of the pyridinium cation, that behaves as stronger electron-withdrawing group, and a C=C spacer, which allows a better conjugation inside the molecule with respect to an azo spacer.¹⁸ Moreover chemical, physical and photochemical stabilities should be substantially the same for **1** and published azo-dyes. The preparation of **1** has been carried out according to Scheme 1.

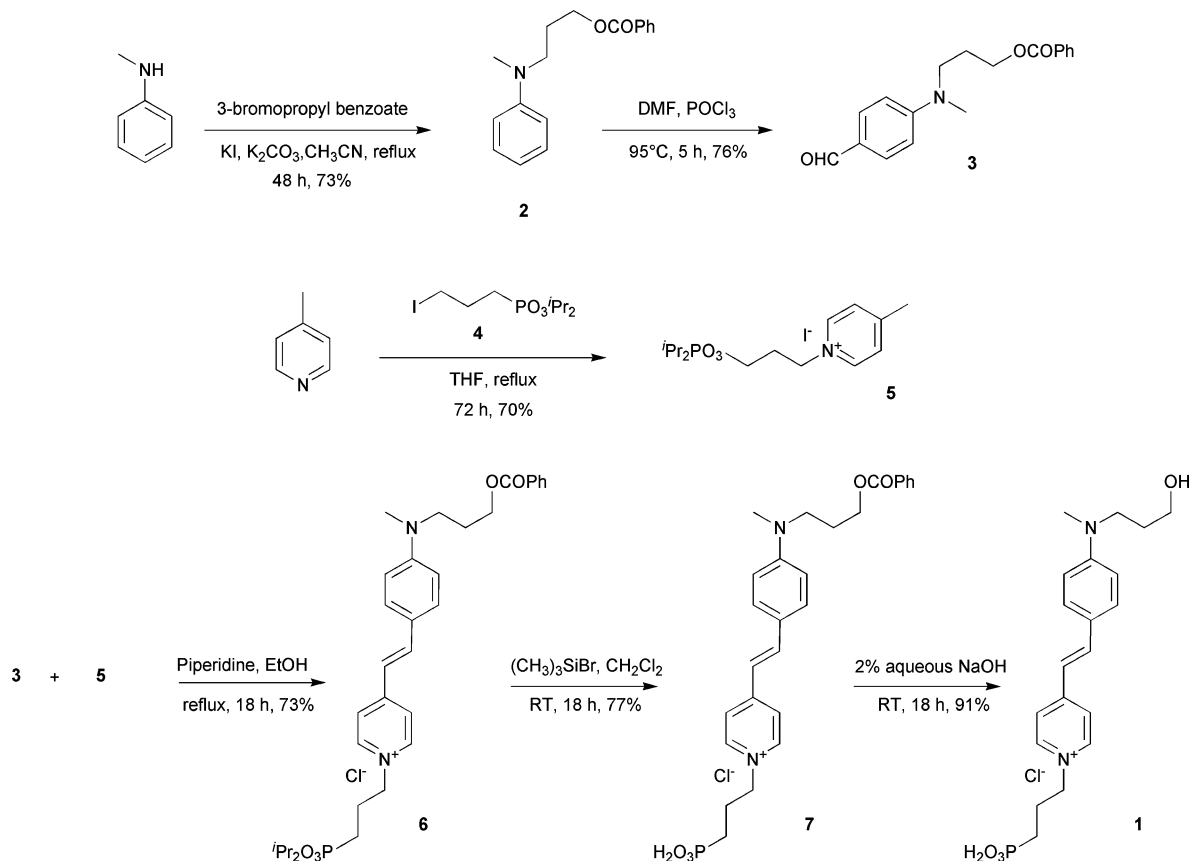
The hydroxyl protected benzaldehyde **3** was prepared in 76% yield by Vilsmeier reaction of *N*-(3-benzoyloxypropyl)-*N*-methylaniline **2**, which was obtained by alkylation of commercially available *N*-methylaniline with 3-bromopropyl benzoate carried out in refluxing CH₃CN in the presence of catalytic amounts of KI and solid K₂CO₃ as base. The pyridinium salt **5** was obtained in 70% yield by alkylation of 4-picoline with 3-iodopropyl phosphonic acid isopropyl ester **4**.¹⁹ The key step of

the synthesis is the condensation of **3** and **5** promoted by piperidine in refluxing ethanol for 18 h, which afforded the completely protected stilbazolium salt **6** in 73% yield after purification by column chromatography. Stilbazolium salt **1** was readily obtained from **6** through two subsequent hydrolysis steps. The cleavage of phosphonic ester was achieved by treatment of **6** with trimethylsilyl bromide in CH₂Cl₂ afforded the benzoyl protected derivative **7** in 77% yield. This latter was hydrolyzed with aqueous 2% NaOH to give **1** in 91% yield after purification with Amberlite XAD 1600T in order to remove all inorganic salts.

The simultaneous removal of both protecting groups is also possible by treating **6** with concentrated hydrochloric acid at 70 °C overnight and subsequent purification with Amberlite XAD 1600T.

Preparation of multilayer films by the Zr-PO_x technique

The protocols reported in the literature for the preparation of Zr-PO_x multilayer films seem all very similar, but a careful insight of the experimental procedures evidences deep differences concerning mostly the priming of the surface and the reaction conditions used (solvents, temperatures, pH, reaction times and so on). The aim of the priming step is to produce a properly functionalized surface monolayer from which the chemisorption-based film deposition can be initiated. In the case of the Zr-PO_x assembly technique the primed surface consists of a Zr⁴⁺ phosphate or phosphonate monolayer. The priming of hydroxyl groups containing surfaces used by Katz and co-workers was carried



Scheme 1 Synthesis of push-pull stilbazolium salt **1**.

out by treating the substrate with 3-aminopropyltrimethoxysilane, phosphorylation of the amino-terminated monolayer with POCl_3 and subsequent zirconation of the resulting phosphoramidate end groups.¹² In our protocol the priming of substrate has been carried out directly reacting the superficial hydroxyl groups with POCl_3 and the so-obtained phosphate residues zirconated with ZrOCl_2 (Fig. 1). In this way it was possible to avoid the drawbacks associated with the very high reactivity of 3-aminopropyltriethoxysilane¹² that requires strictly controlled reaction conditions in order to avoid undesired polymerization on the surface.

Dipping the primed substrate in a 1.5 mM aqueous solution of stilbazolium salt **1** at pH 2–3, adjusted by addition of 10% aqueous HCl, for 15 min at 70 °C led to formation of the first monolayer by reaction of the phosphonic acid end group of **1** with the superficial Zr^{4+} phosphate. Layered zirconium phosphate phosphonate salts are normally prepared by simple precipitation reaction in which a source of Zr^{4+} cations is mixed with a solution of the appropriate organic phosphoric or phosphonic acid. Since the reaction involves the loss of protons from weak acids this step is pH dependent.¹⁷ Indeed the optimum pH for the chemisorption step is in the range 2–3 because the phosphoric or phosphonic acid groups are dissociated and ligating at this pH where the metal ions are Lewis acidic. In order to maintain the optimum conditions we believe that water is the best solvent for the chemisorption of the chromophore although EtOH,²⁰ dimethylacetamide–EtOH,¹⁹ DMF–EtOH²¹ and DMSO²² have been used as solvents. Although push–pull molecules, because of the strong repulsion between dipoles, should spontaneously array in a centrosymmetric arrangement, the strong reactivity of Zr(IV) towards phosphonate groups of **1** precluded this phenomenon. A modified procedure with respect of the priming step was used in phosphorylation of hydroxyl groups of the anchored NLO

molecules. In this case the substrate was transferred into a 20 mM POCl_3 and 20 mM collidine acetonitrile solution for 10 min at room temperature and then rinsed with CH_3CN and water. Each monolayer was considered completed after the zirconation step, which ensured the capping of the organic/inorganic lamellar structure, thus avoiding possible molecular reorientation in the chromophore layer. It is worth stressing that with glass quartz substrate the growth of the multilayer occurs at both faces of the sample.

Structural characterization of the films

Mass spectrometry. Time of Flight Secondary Ion Mass Spectrometry (ToF-SIMS) analysis has been used at the beginning of this work in order to verify the monolayer formation by investigating the surface after each deposition step.

The positive secondary ion mass spectrum (acquired in “static” conditions) after deposition of the chromophore showed a clear peak at m/z 391 for $(\mathbf{1})^+$ together with several fragmentation peaks (Fig. 2).

After the phosphorylation step the same behavior was observed in the case of a phosphonate monolayer, where the occurred reaction on the substrate was confirmed by the presence of a positive peak at m/z 457 for a $(\text{C}_{20}\text{H}_{25}\text{O}_2\text{N}_2\text{P}_2\text{Cl}_2)^+$ fragment in addition to a number of other phosphorylated species. Interesting information was collected by analysis of the negative secondary ions mass spectrum (Fig. 3), which evidenced the presence of a characteristic pattern due to repetitive losses of $(\text{C}_4\text{H}_9\text{NO}_4\text{P})^+$ fragments of m/z 166 Da. This gives evidence of the presence on the surface of sufficiently large domains in which the chromophore molecules are tightly packed.

Similar mass spectra have been obtained also during the preparation of subsequent monolayers thus indicating that the

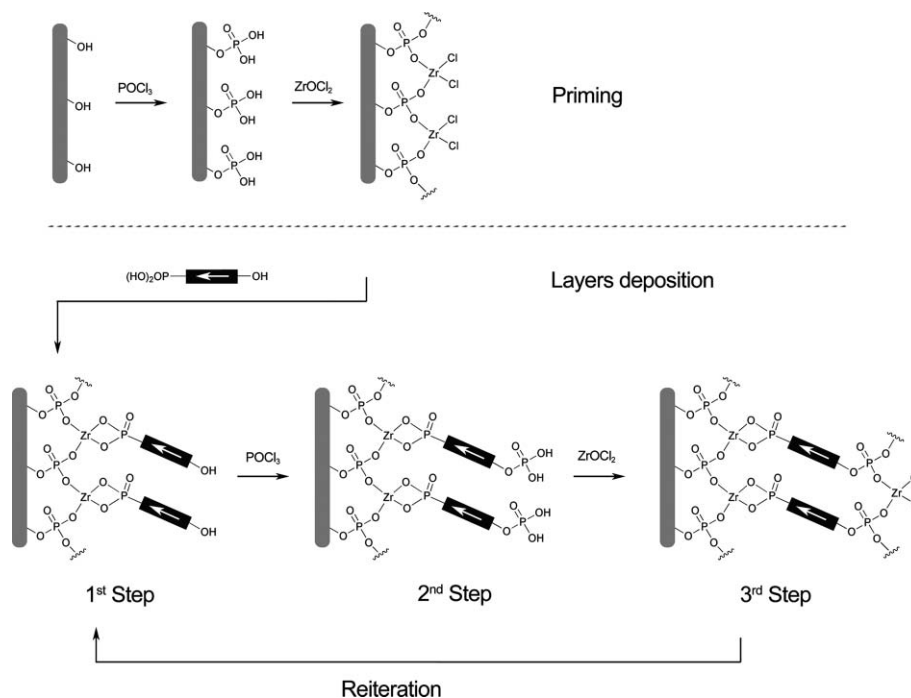


Fig. 1 Schematic representation of adopted deposition protocol.

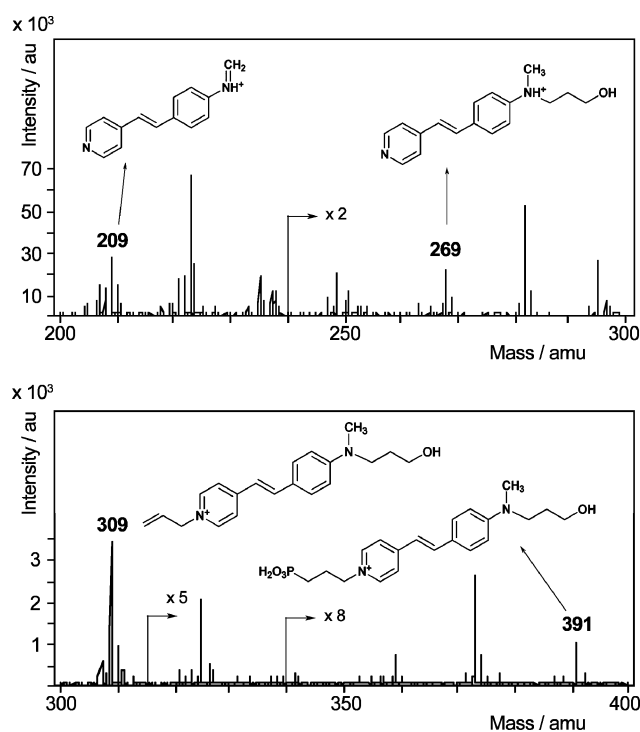


Fig. 2 Part of a typical positive ToF-SIMS spectrum of the molecular film after the first chromophore adsorption.

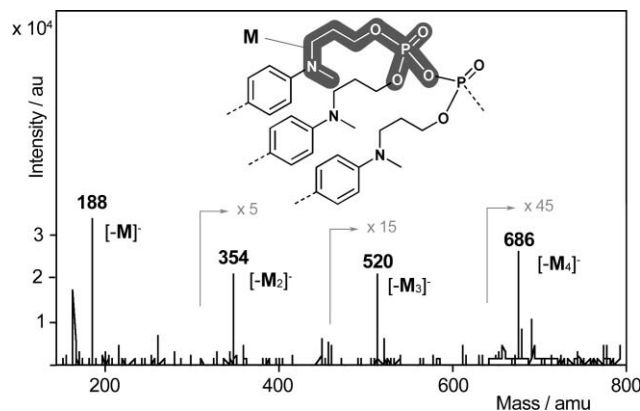


Fig. 3 Portion of the negative ion ToF-SIMS spectrum of the phosphorylated layer.

reaction occurring at each step is highly reproducible. Dual-beam ToF-SIMS depth profiles have been acquired in order to obtain indirect evidence of the multilayer growth. Such profiles are obtained by sputtering the surface with a relatively large current ion beam and analyzing the crater bottom by a second ion beam. In the obtained depth profiles the molecular information from the organic layer is lost, due to the extensive ion beam-induced damage of the organic system occurring in depth profiling conditions (dynamic SIMS). However the elemental signals are still present and can be followed as a function of the number of sputter cycles (proportional to the sputter time and also to the film thickness under the assumption of constant sputter rate).

In particular we used the rise of the Si^+ signal from the substrate for locating the interface in samples of different thickness. By following this signal as a function of sputter cycles it is possible to extract indirect evidence of the film growth (Fig. 4). Indeed the

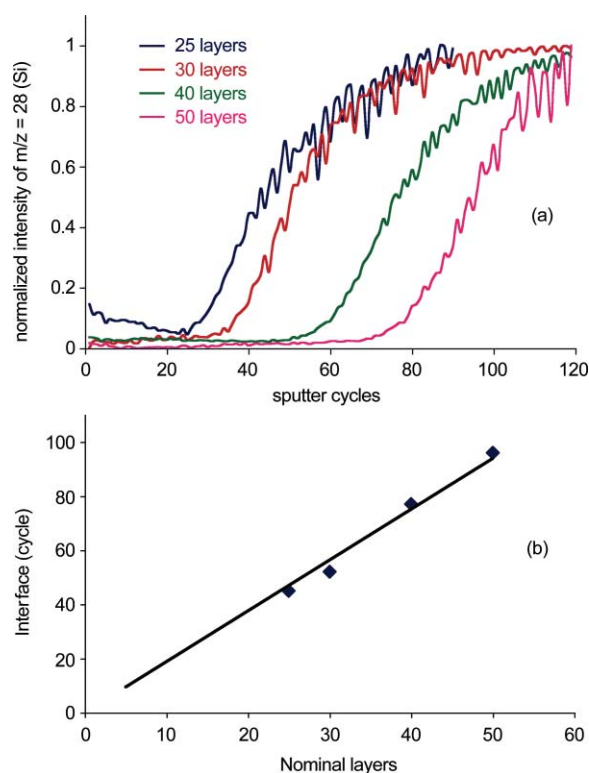


Fig. 4 (a) Typical ToF-SIMS profiles of Si^+ signal acquired on chromophore multilayers of different thickness. (b) Number of sputter cycles necessary for reaching the interface as a function of chromophore nominal number of layers. The position of the interface is obtained from the inflection point of profiles in (a).

inflection point of the sigmoidal curve of the Si^+ signal indicates the point where all the deposited film has been removed and the naked quartz surface is reached by the sputtering ion beam. The good linearity observed in Fig. 4(b) indicates that the thickness of the film under investigation is directly proportional to the number of layers and is a further proof of the reproducibility of this deposition technique.

UV-Vis Analysis. UV-Vis spectroscopy is the simplest analytical technique that allows to follow the growth by measuring the absorption of the multilayers. Indeed a linear increase of the absorbance by increasing the number of layers indicates that a constant amount of chromophore is anchored to the substrate after each deposition cycle. Fig. 5(a) shows the UV-Vis absorption spectrum of chromophore **1** in 4.37×10^{-5} M aqueous solution together with those of four samples having 10, 20, 30 and 35 layers, respectively.

The absorption profile of the chromophore **1** in aqueous solution is characterized by a large maximum at 461 nm, probably influenced by a relevant charge-transfer contribution between the electron-withdrawing and electron-donating groups. This peak shifts to 476 nm in the case of the push-pull molecule fixed to the quartz surface, indicating the possible formation of J-aggregates of **1** within the monolayer. Indeed when polar compounds are packed in a monolayer strong interactions occur between molecules thus allowing the formation of aggregates which are characterized by a blue-shift (H-aggregates) or by a red shift (J-aggregates).^{23,24} Furthermore an increasing absorption in the UV range can be

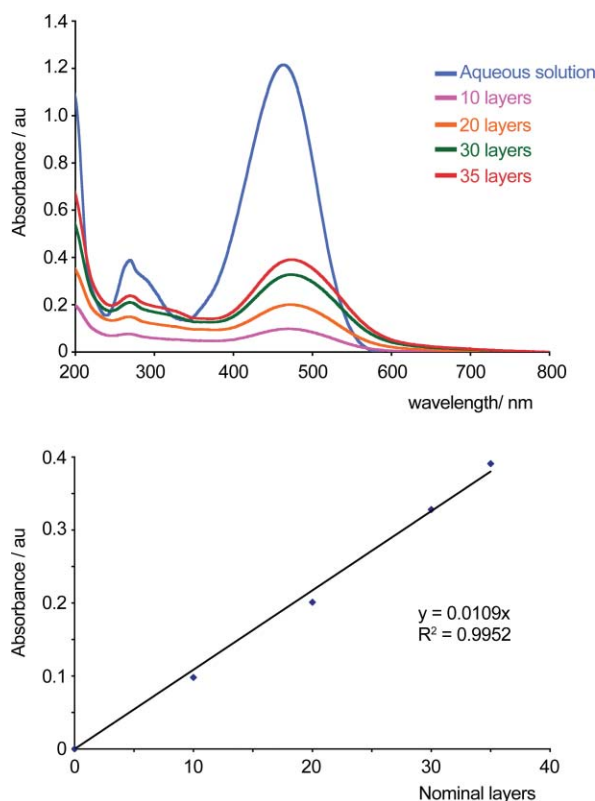


Fig. 5 (a) UV-Vis absorption spectra of **1** in aqueous solution and of multilayer samples; (b) absorbance of multilayer samples plotted vs nominal layers.

envisaged that is due to the presence of the inorganic layers. Fig. 5(b) shows a plot of the absorption maximum of the four multilayer samples of Fig. 5(a) as a function of the number of layers. The linear dependence of the absorption from the number of layers evidences that the single layer deposition is highly reproducible in the deposition of the multilayer film. The slope of the best fit line through the origin was 0.0109 per layer which corresponds to the mean absorption of the single layer. We have also estimated the molar extinction coefficient for our chromophore at the maximum of absorbance in aqueous solution giving a value of $27820 \text{ l cm}^{-1} \text{ mol}^{-1}$. From the mean single layer absorption and the chromophore molar extinction coefficient value, it is possible to calculate the surface chromophore density σ by the expression:

$$\sigma = m_{\text{abs}} N_{\text{A}} / 1000\epsilon \quad (1)$$

where m_{abs} (layer^{-1}) is the slope of the line obtained by plotting absorption maxima vs nominal layer numbers, and N_{A} is Avogadro constant. We obtained a value for σ of $2.36 \times 10^{14} \text{ molecules cm}^{-2} \text{ layer}^{-1}$, which is comparable with values reported in the literature for Zr- PO_x films of some azo-dyes.²⁰

Atomic force microscopy (AFM) analysis

1 mm \times 1 mm AFM micrographs of samples having 10 and 35 layers of **1** are shown in Fig. 6(a) and (b).

The images show similar topographies with no evidence of cracks or pinholes. The surfaces appear relatively homogeneous although the average roughness obtainable from these images is

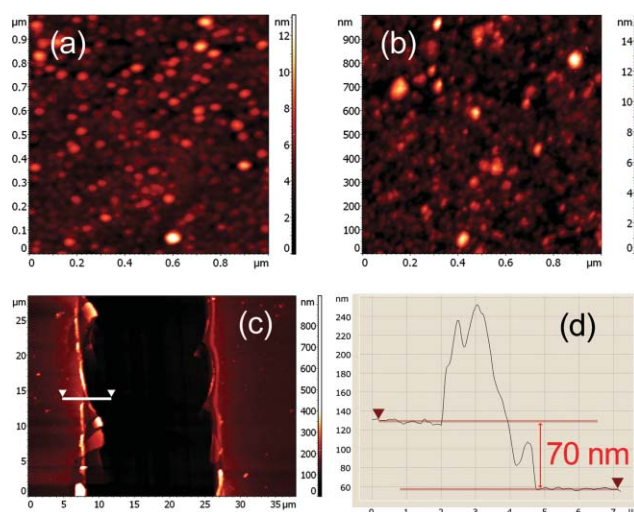


Fig. 6 1 $\mu\text{m} \times 1 \mu\text{m}$ AFM images of samples having 10 (a) and 35 (b) layers. Also shown are an AFM image of a scratched 35 layer sample (c) and measurement of the corresponding thickness (d).

affected by the presence of aggregates with height in the range 12–15 nm, probably due to adventitious precipitation of insoluble zirconium salts occurring during the multilayer deposition process.²³ Comparing the surface morphologies of the two samples, the 35-layer sample seems to have more extended homogeneous areas together with fewer zirconium salt aggregates, although they seem to be larger. By scratching the surface with a metallic tip it is possible to completely remove the multilayer Zr- PO_x film from the quartz surface as shown in Fig. 6(c). It should be stressed that the complete detachment of the film occurs only with difficulty with in general the Zr- PO_x film of the chromophore **1** being very compact and showing good adherence to the quartz surface. This observation is also proved by the presence of vitreous chips well evidenced at the border of the scratch. Fig. 6(d) shows the cross section profile obtained by the AFM tip along the white line shown in Fig. 6(c). The highest peak of this profile near to the border of the scratch is due to the removed material, while the roughness of the surface seems to be very low. The cross section measurement indicates that the thickness of the 35-layer film is 70 nm.

From this value and from ellipsometric measurements carried out on several samples having different numbers of layers an average thickness of 2 nm per monolayer could be obtained. By considering that the thickness of the Zr- PO_x inorganic layer obtained by crystallographic data is 0.7 nm,¹⁴ the length of the chromophore **1** is 2 nm (molecular mechanic calculations) and that the average thickness of the multilayer is 2 nm, the tilt angle calculated for the multilayer samples is 50° , a value very close to that (46°) reported in the literature for a similar azo-dye.²¹

Second harmonic generation (SHG) measurements

The SHG signal of the same series of films, from 10 to 35 layers, was measured with the experimental set up described in the following section. The Maker fringes for the 35-layer film (Fig. 7) were integrated and the subtending areas plotted as function of the number of layers.

As it was supposed the signals were quadratically proportional to the number of layers (Fig. 8) and it follows that the square

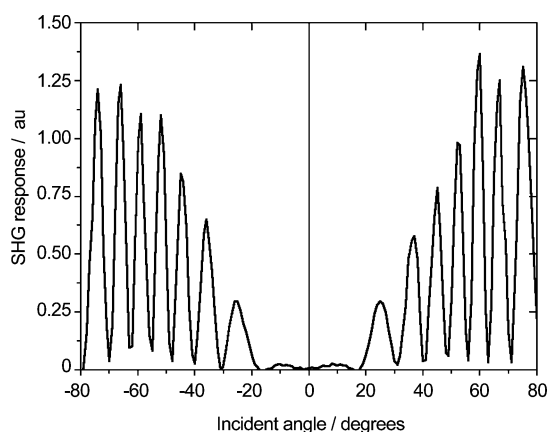


Fig. 7 Example of SHG angle dependence intensity response for a 35-layer zirconium phosphate/phosphonate film.

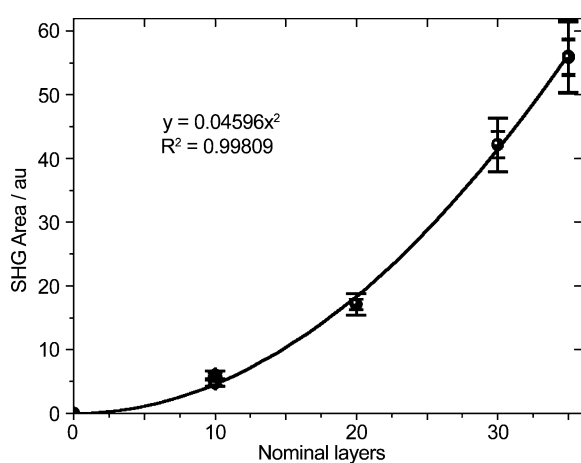


Fig. 8 SHG integrated area plotted vs. nominal layers.

root of areas increases linearly (Fig. 9). This result was in accord with the linear growth of the absorption spectra and it suggested a good reproducibility of deposition technique and a constancy of polar order of chromophores even after several layer depositions. The second-order NLO properties of bulk materials are generally defined by the susceptibility tensor χ_{IJK}^2 . For second harmonic generation (SHG) and optical rectification it is a common practice

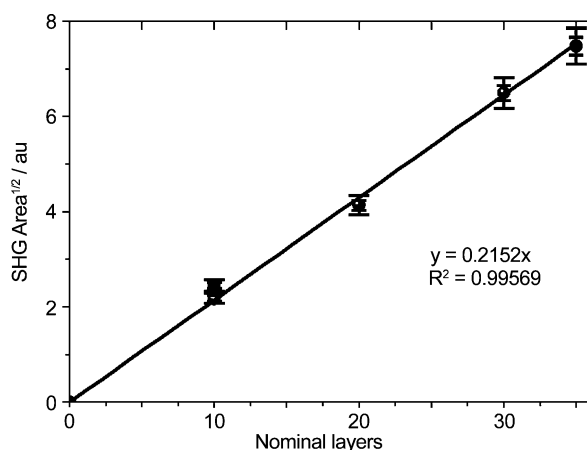


Fig. 9 Square-root of SHG integrated area plotted vs. nominal layers.

to write the induced non-linear polarization in terms of the tensor d_{IJK} which is related to the second-order susceptibility by eqn (2).⁸

$$d_{IJK} = 0.5\chi_{IJK}^2 \quad (2)$$

In this equation IJK indices represent the coordinate system of the bulk material. Tensor d components were calculated by fitting experimental curves collected for three different polarizations (see Experimental section). For the system under investigation only three of the d tensor elements are non-zero: d_{15} , d_{31} and d_{33} . The values of d_{15} and d_{31} could be obtained directly through two different measurements in SP→S and SS→P polarization configuration, respectively. These values were then used to calculate d_{33} which represent the SHG values along the direction perpendicular to the sample surface (z axis).

A mean d_{33} value of 12 pm V⁻¹ was found and the results were in good agreement for all films. This value was comparable to that obtained by Katz *et al.* (19 pm V⁻¹) for a similar chromophore and is in the range of those found for LiNbO₃ (2–44 pm V⁻¹).²⁵

As it is evidenced in Fig. 10 the d_{33} values obtained for samples of 10, 20, 30 and 35 layers are all very similar and fall within the error bars, thus giving further evidence that the deposition technique ensures a regular orientation of chromophores by increasing the number of layers.

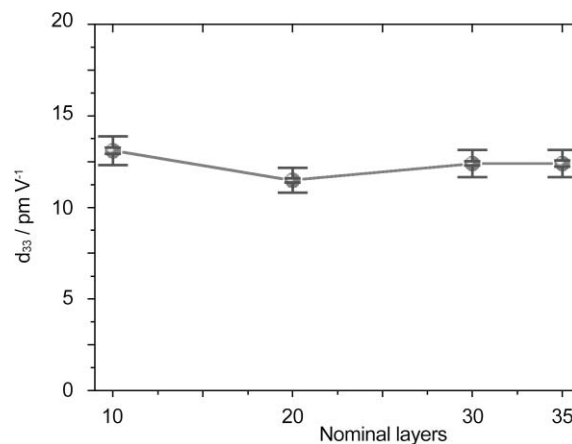


Fig. 10 d_{33} (pm V⁻¹) vs. nominal layers.

Experimental

Materials and methods

All commercially available solvents and reagents were used as received. TLC was carried out on silica gel Si 60-F254. Column chromatography was carried out on silica gel Si 60 mesh size 0.040–0.063 mm (Merk, Darmstadt, Germany). ¹H NMR spectra were recorded with a Bruker AC300 spectrometer operating at 300 MHz. UV-Vis spectra were recorded on Nicolet Evolution 500 (Thermo Electron Corporation) spectrometer, ellipsometric measurements were carried out at CIVEN laboratories with a GES 5 (Sopra) ellipsometer and AFM images were obtained from NTEGRA Probe NanoLaboratory (NT-MDT) microscope. ToF-SIMS measurements were performed with ToF-SIMS IV (ION-ToF, Muenster, Germany) instrumentation. Static SIMS spectra were obtained with ⁶⁹Ga⁺ primary ions (25 keV, PI fluence < 3 × 10¹¹ ions cm⁻²). Depth profiles were obtained in dual beam mode,

using Ar⁺ ions (1 keV) for sputtering and ⁶⁹Ga⁺ (25 keV) for analysis. The sputter beam (1020 nA) was rastered over 500 mm × 500 mm, and the analysis beam (1 pA) over a concentric area of 100 mm × 100 mm. A slow (18 eV) pulsed electron flood was used for charge compensation when acquiring profiles from insulating samples. Determination of second-order coefficients was performed by the Maker fringes technique.²⁶ Second harmonic generation (SHG) measurements of samples were carried out with a Q-switched Nd:YAG (Quanta System HYL-101) laser operating at 1064 nm, 10 Hz repetition rate. The laser intensity on the sample was measured by a pyroelectric detector Gentec-eo QE25SP-S-MB and was about 0.2 mJ pulse⁻¹. The light beam was focalized on the sample by a 400 mm lens. The focus was positioned a few millimeters in front of the sample to avoid damage to the films. The polarization of the incident beam was controlled by a λ/2 waveplate. Polarization of a duplicated beam was selected by a beam-splitter polarizer cube mounted on a rotation stage.

The samples were mounted on a motorized rotation stage Newport SR50. The rotation stage was controlled by a Newport ESP300 motion driver. Care was taken to make the incident beam to precisely pass through the rotation axis; the minimum step resolution available was 0.001°. The second harmonic signals intensity (532 nm) was measured by a H9307-03 Hamamatsu photomultiplier (PMT) connected to a Tektronix 3054B oscilloscope. A visible interference filter (centre wavelength 532 nm) was mounted in front of the PMT to remove the infrared transmitted fundamental beam and to reveal just second harmonic (SH) signals.

In order to take in to account both films on the opposite side of the quartz substrate and to obtain the NL coefficients a modified Hermann & Hayden formula²⁷ was used for interpreting the SHG phenomenon in nonzero absorption films. To correctly calculate the angular dependence of the signal it was necessary to consider the difference of phase between the beams generated in the two different layers on both faces of the substrate. This difference of phase Δφ depends on both the thickness and the light dispersion of the substrate and can be written as:

$$\Delta\phi_s = (2\omega L_s / c) (n_s^{2\omega} \cos\theta_s^{2\omega} - n_s^\omega \cos\theta_s^\omega) \quad (3)$$

where n^ω and $n^{2\omega}$ are the refractive indexes for the fundamental and the duplicate frequencies in the substrate and θ^ω and $\theta^{2\omega}$ are the propagation angles of the two beams inside the quartz.

Accordingly the SH intensity could be defined by the expression:

$$P_{\text{TOT}}^{2\omega} = P_1^{2\omega} + P_2^{2\omega} + 2\sqrt{P_1^{2\omega}P_2^{2\omega}} \cos\Delta\phi_s \quad (4)$$

where $P_{\text{TOT}}^{2\omega}$ is the power of SHG signal detected by the PMT, $P_1^{2\omega}$ and $P_2^{2\omega}$ is the power of second harmonic generated at the front and back faces of the sample. As a matter of fact $P_{\text{TOT}}^{2\omega}$ is strongly angle dependent and the number and the position of the minima are strictly related to the thickness of the quartz substrate. The Maker fringes technique needs a well-known reference to calculate NL coefficients. For this reason a quartz crystal wafer (X-cut 1 mm thick, d_{11} is 0.46 pm V⁻¹^{28,29}) was used as reference. The presence of a reference substrate was also necessary for completely removing the laser beam power long term drift and to take in account the beam waist width. Thus the Maker fringes measurement of the reference was performed just before each measurement. Short-term power fluctuations were reduced by choosing an adequate averaging time.

For calculation of the absolute value of the second-order NLO coefficient, the punctual symmetry of the multilayer films was assumed to be $C_{\infty v}$. This was reasonable in consideration of deposition technique and of literature references,³⁰ and was also confirmed by experimental evidences. For a $C_{\infty v}$ system only three of the tensor elements are nonzero: d_{15} , d_{31} and d_{33} . The values of d_{15} and d_{31} could be obtained directly through two different measurements in SP→S and SS→P polarization configuration, respectively. These values were then used to calculate the value of the d_{33} tensor from PP→P configuration measurement. In order to correctly construct a theoretical model to fit the experimental data it was necessary to evaluate the linear optical properties of the material and this was done by performing UV-Visible absorption spectra (Perkin-Elmer Lambda 2 Spectrometer) and ellipsometric measurement (GES 5-Sopra) in the 200–1100 nm range. As mentioned previously the theoretical model was constructed starting from the assumptions of Herman and Hayden.²⁷

N-Methyl-*N*-(3-benzoyloxypropyl)aniline (2)

Solid potassium iodide (0.85 g, 5.1 mmol) and potassium carbonate (7.07 g, 51.2 mmol) were added to a solution of *N*-methylaniline (1.37 g, 12.8 mmol) and 3-bromopropyl benzoate (3.42 g, 14.1 mmol) in acetonitrile (50 mL) and the mixture was refluxed under magnetic stirring for 48 h. The mixture was cooled at room temperature, diluted with acetonitrile (50 mL), filtered on a fritted glass and the filtrate was evaporated to afford a residue. This product was dissolved in dichloromethane (100 mL) and washed with water (2 × 50 mL). The organic phase, dried over magnesium sulfate, was evaporated under reduced pressure to afford an orange oil residue which was purified by column chromatography on silica gel using 6 : 4 (v/v) light petroleum–dichloromethane as eluent to afford **2** (2.51 g, 73%) as a colourless oil; δ_{H} (200 MHz, CDCl₃) 8.06 (2H, m), 7.49 (1H, m), 7.45 (2H, m), 7.22 (2H, m), 6.71 (3H, m), 4.38 (2H, t, *J* 6.23), 3.52 (2H, t, *J* 7.11), 2.96 (3H, s), 2.06 (2H, quintet, *J* 7.01).

3-[(4-Formylphenyl)(methylamino)propyl benzoate (3)

A mixture of anhydrous dimethylformamide (30 mL) and POCl₃ (1.49 g, 9.7 mmol) was stirred under nitrogen atmosphere at 0 °C for 1.5 h, then at room temperature for 1 h to give a yellow solution that was then heated at 95 °C. A sample of *N*-methyl-*N*-(3-benzoyloxypropyl)aniline **2** (2.5 g, 9.3 mmol) dissolved in dimethylformamide (6 mL) was added and the resulting mixture was stirred at 95 °C for 4 h. The solvent was removed under reduced pressure, the residue was taken up with water (50 mL) and the pH was adjusted at 7–8 by addition of sodium bicarbonate saturated aqueous solution, then the organic phase was extracted with *n*-hexane (6 × 50 mL). The organic phase was washed with water (100 mL), dried with magnesium sulfate and the solvent evaporated under reduced pressure to afford a brown oil residue that was purified by column chromatography on silica gel using pure dichloromethane first and subsequently dichloromethane–ethyl acetate 10 : 0.3 (v/v) as eluent to afford **3** (2.11 g, 76%) as a colourless oil; δ_{H} (200 MHz, CDCl₃) 9.73 (1H, s), 8.03 (2H, m), 7.74 (2H, d, *J* 9.00) 7.60 (1H, m), 7.47 (2H, m), 6.74 (2H, d, *J* 1.0), 4.39 (2H, t, *J* 6.09), 3.63 (2H, t, *J* 7.12), 3.09 (3H, s), 2.11 (2H, quintet, *J* 7.48).

1-[3-(Diisopropoxyphosphoryl)propyl]-4-methylpyridinium iodide (5)

A solution of diisopropyl 3-iodopropyl phosphonate (**4**) (1.82 g, 5.4 mmol) and 4-methylpyridine (0.81 g, 8.7 mmol) in anhydrous tetrahydrofuran (20 cm³) was heated at reflux for 72 h. The mixture was cooled at room temperature and the solvent evaporated to dryness under reduced pressure to afford a deep yellow thick oil. This product was stirred overnight with diethyl ether (40 cm³) to afford a solid that was filtered on a fritted glass in a nitrogen atmosphere and dried under vacuum to afford **5** (1.62 g, 70%) as a yellow hygroscopic solid; δ_{H} (200 MHz, CDCl₃) 9.33 (2H, d, *J* 6.70), 7.85 (2H, d, *J* 6.50), 5.08 (2H, t, *J* 7.18), 4.68 (2H, m), 2.69 (3H, s), 2.40 (2H, m), 1.76 (2H, m), 1.32 (12H, d, *J* 6.20).

(*E*)-4-{4-[3-(Benzoyloxypropyl)(methylamino)styryl]-1-[3-(diisopropoxyphosphoryl)propyl]pyridinium chloride (6)

A solution of **5** (3.68 g, 12.4 mmol), **3** (3.73 g, 12.37 mmol) and 20 drops of piperidine in ethanol was heated at reflux for 18 h. The mixture was cooled at room temperature and the solvent evaporated to dryness under reduced pressure to afford a residue that was purified by column chromatography using 9 : 1 (v/v) dichloromethane–methanol as eluent to give pure **6** (4.72 g, 70%) as orange powder; δ_{H} (CDCl₃, 300 MHz) 9.04 (2H, d, *J* 6.83), 8.04 (2H, d, *J* 7.23), 7.80 (2H, d, *J* 6.86), 7.59 (2H, m); 7.47 (4H, m), 6.84 (1H, d, *J* 15.9), 6.73 (2H, d, *J* 8.9), 4.87 (2H, t, *J* 7.02), 4.67 (2H, m), 4.39 (2H, t, *J* 6.07); 3.61 (2H, t, *J* 7.01), 3.08 (3H, s), 2.34 (2H, m), 2.11 (2H, quintet, *J* 6.62), 1.77 (2H, m), 1.32 (12H, d, *J* 6.20).

(*E*)-4-{4-[3-(Benzoyloxypropyl)(methylamino)styryl]-1-(3-phosphonopropyl)pyridinium chloride (7)

A solution of **6** (4.72 g, 6.68 mmol) and trimethylsilyl bromide (3.68 g, 24.05 mmol) in 40 ml of anhydrous CH₂Cl₂ was stirred overnight at room temperature and under nitrogen atmosphere. The solvent was evaporated to dryness under vacuum and the residue was dissolved in water (200 cm³) at pH 8.5, by adding a saturated solution of sodium carbonate, to afford a deep red solution. This solution was washed with diethyl ether (2 × 70 cm³) and acidified at pH 3–4 by addition of 10% aqueous hydrochloric acid to afford a solid precipitate which was filtered on a fritted glass, washed with dioxane (50 cm³) and dried under vacuum to give 2.74 g (77%) of product as red powder; δ_{H} (CD₃OD, 200 MHz), 8.62 (2H, d, *J* 6.86), 8.01 (4H, m), 7.82 (2H, d, *J* 16.03), 7.54 (5H, m), 7.06 (2H, d, *J* 15.99), 6.81 (2H, d, *J* 8.98), 4.52 (2H, t, *J* 7.29), 4.38 (2H, t, *J* 6.04), 3.67 (2H, t, *J* 7.09), 3.08 (3H, s), 2.14 (4H, m), 1.55 (2H, m).

(*E*)-4-{4-[3-(Hydroxypropyl)(methylamino)styryl]-1-(3-phosphonopropyl)pyridinium chloride (1)

A solution of **7** (0.806 g, 1.3 mmol) in 2% sodium hydroxide aqueous solution (30 cm³) was stirred overnight at room temperature. The solution was adjusted at pH 7–8 by addition of 10% aqueous hydrochloric acid and the product was purified by column chromatography on Amberlist XAD 1600T by eluting the inorganic salts with pure water and the product with 8/2 (v/v) water/acetonitrile. Evaporation of the solvent afforded 0.61 g

(91%) of pure product **1** as a red powder (Found: C, 55.7; H, 6.8; N, 6.6. C₂₀H₂₈N₂O₄P requires C, 56.3; H, 6.6; N, 6.6); δ_{H} (CD₃OD, 300 MHz) 8.63 (2H, d, *J* 6.88), 7.93 (2H, d, *J* 6.89), 7.79 (1H, d, *J* 15.98), 7.58 (2H, d, *J* 8.93), 7.05 (1H, d, *J* 16.01), 6.79 (2H, d, *J* 8.98), 4.51 (2H, t, *J* 7.36), 3.62 (2H, t, *J* 6.08), 3.55 (2H, t, *J* 7.27), 3.05 (3H, s), 2.20 (2H, m), 1.82 (2H, quintet, *J* 7.05), 1.48 (2H, m); *m/z* (ToF-SIMS) 391 (M⁺. C₂₀H₂₈N₂O₄P requires 391); λ_{max} (EtOH): 488 nm ($\epsilon/\text{dm}^3 \text{ mol}^{-1} \text{ cm}^{-1}$ 36 996); λ_{max} (H₂O)/nm 461 ($\epsilon/\text{dm}^3 \text{ mol}^{-1} \text{ cm}^{-1}$ 27 820).

Film preparation

Layers were deposited on quartz glass HSQ 300 which surfaces were cleaned and oxidized by immersion for 15 min at 60 °C in a freshly prepared Piranha solution (3 : 1 mixture of 96% H₂SO₄ and 30% H₂O₂), followed by rinsing with deionized water for 5 min and drying under a nitrogen stream. **CAUTION!** a mixture of concentrated sulfuric and hydrogen peroxide reacts violently with many organic compounds and should be handled with care. The hydroxyl-functionalized surface was then immersed in neat POCl₃ at room temperature for 18 h, washed with acetonitrile and water and dried under nitrogen stream to convert –OH groups into –OPO(OH)₂ residues. The deposition of a Zr(IV) layer was achieved by immersion of the substrate in a 5 mM ZrOCl₂·8H₂O aqueous solution at room temperature for 10 min. Again the substrate was rinsed by dipping into deionized water for 5 min and dried under a nitrogen stream to complete priming procedure. The formation of the first monolayer of chromophore **1** was fulfilled by dipping the sample in a 1.5 mM aqueous solution of the stilbazolium salt **1** at pH value, adjusted by addition of 10% HCl, in the range 2–3 for 15 min at 70 °C. After careful washing with water for 5 min the substrate was transferred into a 20 mM POCl₃ and 20 mM collidine acetonitrile solution for 10 min at room temperature and then rinsed with CH₃CN and water. The third step of deposition was accomplished again by immersion of substrate into a 5 mM ZrOCl₂·8H₂O aqueous solution at room temperature for 10 min. Each deposition cycle was considered completed after the zirconation step, which ensured the capping of the organic/inorganic lamellar structure, thus avoiding possible molecular reorientation in the chromophore layer. It is worth stressing that with glass quartz substrate the growth of the multilayer occurs at both faces of the sample.

Conclusions

The results here reported indicate that the Zr-PO₃ technique represents a useful way to nanorganize push–pull NLO active molecules into multilayered inorganic–organic thin films in which the polar order is ensured by the design of the chromophore. Indeed only the phosphonate end of the chromophore can be chemisorbed by the zirconium phosphate primed surface of the substrate leaving the hydroxyl ended part available for the regeneration of the surface through two simple chemical steps, *i.e.* phosphorylation and zirconation. Although the steps required for the preparation of each monolayer are very simple, the optimization of the deposition conditions, namely solvent, pH, temperature and time of reaction, proved to be very important in determining the homogeneity and the chemical–physical properties of the obtained materials. Another important point rests on the careful chemical

characterization of the surface during the preparation of the multilayer in order to guarantee the reproducibility of the steps allowing the formation of each monolayer. Taking care of these considerations and by using the Zr-PO_x technique it has been possible to prepare highly homogeneous and reproducible thin films of the stilbazolium salt **1**, that are characterized by superior mechanical stability and NLO properties. The results obtained clearly evidence the great potential of the ZrPO_x assembly technique for the preparation of multilayered films in which a defined alignment of molecules should be maintained. An important aspect which needs to be investigated is the possibility of automating the layer by layer deposition thus allowing the preparation of micrometer thick films that are often required for NLO operating devices. Further investigations aimed to use the Zr-PO_x technique for the assembly of new and more active chromophores are under way in our laboratories.

Acknowledgements

T. M. and V. C. thank MIUR FIRB 2001 “Nanorganization of hybrid organo–inorganic molecules with magnetic and non-linear optical properties” and MIUR FIRB RBNE033KMA “Molecular compounds and hybrid nanostructured materials with resonant and non-resonant optical properties for photonic devices” for financial support. Convenzione “PROMO” CNR-INSTM entitled “Nanostrutture organiche, organometalliche, polimeriche e ibride: ingegnerizzazione supramolecolare delle proprietà fotoniche e dispositivistica innovativa per optoelettronica” is also acknowledged for supporting this research.

Notes and references

- 1 A. Dowling, R. Clift, N. Grobert, D. Hutton, R. Oliver, O. O'Neill, J. Pethica, N. Pidgeon, J. Porritt, J. Ryan, A. Seaton, S. Tandler, M. Welland and R. Whatmore, *Nanoscience and Nanotechnology: Opportunities and uncertainties*, A Report of the Royal Society & The Royal Academy of Engineering, London, July 2004.
- 2 G. M. Whitesides, *Small*, 2005, **1**, 172.
- 3 J. Zyss, *Molecular Nonlinear Optics: Materials, Physics and Devices*, Academic Press, Boston, MA, 1994.
- 4 M. Blanchard-Desce, S. R. Marder and M. Barzoukas, in *Comprehensive Supramolecular Chemistry*, ed. D. N. Reinhoudt, Pergamon Press, New York, 1996, vol. 10, p. 833, and references therein.
- 5 S. R. Marder, J. W. Perry and C. P. Yakymyshyn, *Chem. Mater.*, 1994, **6**, 1137.
- 6 A. N. Rashid, K. Kirschbaum and R. K. Shoemaker, *J. Mol. Struct.*, 2006, **785**, 1.
- 7 M. Ogawa, M. Takahashi and K. Kuroda, *Chem. Mater.*, 1994, **6**, 715.
- 8 D. M. Burland, R. D. Miller and C. A. Walsh, *Chem. Rev.*, 1994, **94**, 31.
- 9 A. Facchetti, E. Annoni, L. Beverina, M. Morone, P. Zhu, T. J. Marks and G. A. Pagani, *Nat. Mater.*, 2004, **3**, 910.
- 10 G. J. Ashwell, *J. Mater. Chem.*, 1999, **9**, 1991.
- 11 G. Decher, *Science*, 1997, **277**, 1232.
- 12 M. E. Van Der Boom, P. Zhu, G. Evmenenko, J. E. Malinsky, W. Lin, P. Dutta and T. J. Marks, *Langmuir*, 2002, **18**, 3704.
- 13 H. E. Katz, *Chem. Mater.*, 1994, **6**, 2227.
- 14 M. B. Dines and P. M. DiGiacomo, *Inorg. Chem.*, 1981, **20**, 92.
- 15 H. Lee, L. J. Kepley, H.-G. Hong and T. E. Mallouk, *J. Am. Chem. Soc.*, 1988, **110**, 618.
- 16 H. Lee, L. J. Kepley, H.-G. Hong, S. Akhter and T. E. Mallouk, *J. Phys. Chem.*, 1988, **92**, 2597.
- 17 G. Cao, H.-G. Hong and T. E. Mallouk, *Acc. Chem. Res.*, 1992, **25**, 420.
- 18 M. J. Lee, M. Piao, M.-Y. Jeong, S. H. Lee, K. M. Kang, S.-J. Jeon, T. G. Lim and B. R. Cho, *J. Mater. Chem.*, 2003, **13**, 1030.
- 19 H. E. Katz, W. L. Wilson and G. Scheller, *J. Am. Chem. Soc.*, 1994, **116**, 6636.
- 20 H. E. Katz, G. Scheller, T. M. Putvinski, M. L. Schilling, W. L. Wilson and C. E. D. Chidsey, *Science*, 1991, **254**, 1485.
- 21 W. C. Flory, S. M. Mehrens and G. J. Blanchard, *J. Am. Chem. Soc.*, 2000, **122**, 7976.
- 22 H. E. Katz, S. F. Bent, W. L. Wilson, M. L. Scilling and S. B. Ungashe, *J. Am. Chem. Soc.*, 1994, **116**, 6631.
- 23 E. Rivera, M. del Pilar Carreón-Castro, I. Buendía and G. Cedilo, *Dyes Pigm.*, 2006, **68**, 217.
- 24 E.-H. Kang, T. Bu, P. Jin, J. Sun, Y. Yang and J. Shen, *Langmuir*, 2007, **23**, 7594.
- 25 S. Singh, in *CRC Handbook of Laser Science and Technology*, ed. M. J. Weber, CRC Press, Boca Raton, FL, 1986, pp. 3–220.
- 26 P. D. Maker, R. W. Terhune, M. Nisenoff and C. M. Savage, *Phys. Rev. Lett.*, 1962, **8**, 21.
- 27 W. N. Herman and L. M. Hayden, *J. Opt. Soc. Am. B*, 1995, **12**, 416.
- 28 J. Jerphagnon and S. K. Kurtz, *Phys. Rev. B: Solid State*, 1970, **1**, 1739.
- 29 R. L. Sutherland, *Handbook of Nonlinear Optics*, Marcel Dekker, New York, 2003.
- 30 M. Eich, H. Looser, D. Y. Yoon, R. Twieg, G. Bjorklund and J. C. Baumert, *J. Opt. Soc. Am. B*, 1989, **6**, 1590.